Anal. Chem. **2005,** *77,* 208−214

Infrared Multiphoton Dissociation of O-Linked Mucin-Type Oligosaccharides

Jinhua Zhang, Katherine Schubothe, Bensheng Li, Scott Russell, and Carlito B. Lebrilla*

Department of Chemistry and School of Medicine, Biochemistry and Molecular Medicine, University of California at Davis, Davis, California 95616

Oligosaccharides are known to play important roles in many biological processes. In the study of oligosaccharides, collision-induced dissociation (CID) is the most common dissociation method to elucidate the sequence and connectivity. However, a disadvantage of CID is the decrease in both the degree and efficiency of dissociation with increasing mass. In the present study, we have successfully performed infrared multiphoton dissociation (IRMPD) on 39 O-linked mucin-type oligosaccharide alditols (both neutral and anionic). CID and IRMPD spectra of several oligosaccharides were also compared. They yielded nearly identical fragment ions corresponding to the lowest energy fragmentation pathways. The characteristic fragmentations of structural motifs, which can provide the linkage information, were similarly presented in both CID and IRMPD spectra. Multistage of CID (MS^3 or MS^4) is commonly needed to completely sequence the oligosaccharides, while IRMPD of the same compounds yielded the fragment ions corresponding to the loss of the first residue to the last residue during a single-stage tandem MS (MS^2). Finally, it is shown that the fragmentation efficiency of IRMPD increases with the increasing size of oligosaccharides.

Glycosylation is the most common form of posttranslational modification. Two types are known depending on their connection to the protein, N- and O-linked. N-linked oligosaccharides have a common core structure and vary primarily in the nonreducing end. O-Linked, excluding glycosaminoglycans and single monosaccharides, have at least eight core structures.[1] The numbers of possible structural combinations provide a great degree of variability, which have posed a specific challenge for the structural elucidation of O-linked oligosaccharides. However, as a class of compounds, O-linked oligosacchardes play key roles particularly as components of mucin glycoproteins in areas as diverse as reproduction and cancer metastasis.

Tandem mass spectrometry (MS^n), in which a precursor ion is mass selected, reacted, or dissociated and the product ions are mass analyzed, has been an essential technique for structural analysis of biomolecules. In the structural elucidation of oligosaccharides, collision-induced dissociation (CID) is the most common method to obtain sequence, connectivity, in some cases, even the linkage, and stereochemistry.[2−8] For CID with Fourier transform ion cyclotron resonance mass spectrometry (FTICR-MS), the most popular technique is sustained off-resonance irradiation CID (SORI-CID).[9] In SORI-CID, the ions undergo acceleration−deceleration cycles throughout the duration of an alternating electrical field pulse and are slowly activated by sequential, inelastic collisions. As a consequence, the lowest energy pathways for decomposition are often attained.[9] SORI-CID has been extensively used for structural analysis of various biopolymers.[10−30]

* Corresponding author. Fax: 1-530-754-5609. Tel: 1-530-752-6364. E-mail: cblebrilla@ucdavis.edu.

(1) Brockhausen, I. *Biochim. Biophys. Acta* **1999**, *1473*, 67−95.
(2) Domon, B.; Muller, D. R.; Richter, W. J. *Org. Mass Spectrom.* **1989**, *24*, 357−359.
(3) Orlando, R.; Bush, C. A.; Fenselau, C. *Biomed. Environ. Mass Spectrom.* **1990**, *19*, 747−754.
(4) Tseng, K.; Lindsay, L. L.; Penn, S.; Hedrick, J. L.; Lebrilla, C. B. *Anal. Biochem.* **1997**, *250*, 18−28.
(5) Weiskopf, A. S.; Vouros, P.; Harvey, D. J. *Rapid. Commun. Mass Spectrom.* **1997**, *11*, 1493−1504.
(6) Konig, S.; Leary, J. A. *J. Am. Soc. Mass Spectrom.* **1998**, *9*, 1125−1134.
(7) Viseux, N.; de Hoffmann, E.; Domon, B. *Anal. Chem.* **1998**, *70*, 4951−4959.
(8) Tseng, K.; Hedrick, J. L.; Lebrilla, C. B. *Anal. Chem.* **1999**, *71*, 3747−3754.
(9) Gauthier, J. W.; Trautman, T. R.; Jacobson, D. B. *Anal. Chim. Acta* **1991**, *246*, 211−225.
(10) Guan, S.; Marshall, A. G.; Wahl, M. C. *Anal. Chem.* **1994**, *66*, 6, 1363−1367.
(11) Hofstadler, S. A.; Wahl, J. H.; Bakhtiar, R.; Ander, G. A.; Bruce, J. E.; Smith, R. D. *J. Am. Soc. Mass Spectrom.* **1994**, *5*, 894−899.
(12) Huang, Y.; Pasa-Tolic, L.; Guan, S.; Marshall, A. G. *Anal. Chem.* **1994**, *66*, 4385−4389.
(13) Senko, M. W.; Speir, J. P.; McLafferty, F. W. *Anal. Chem.* **1994**, *66*, 6, 2801−2808.
(14) Schwartz, B. L.; Bruce, J. E.; Anderson, G. A.; Hofstadler, S. A.; Rockwood, A. L.; Smith, R. D.; Chilkoti, A.; Stayton, P. S. *J. Am. Soc. Mass Spectrom.* **1995**, *6*, 459−465.
(15) Wu, Q. Y.; Vanorden, S.; Cheng, X. H.; Bakhtiar, R.; Smith, R. D. *Anal. Chem.* **1995**, *67*, 2498−2509.
(16) Little, D. P.; Aaserud, D. J.; Valaskovic, G. A.; McLafferty, F. W. *J. Am. Chem. Soc.* **1996**, *118*, 9352−9359.
(17) Solouki, T.; Pasa-Tolic, L.; Jackson, G. S.; Guan, S.; Marshall, A. G. *Anal. Chem.* **1996**, *68*, 3718−3725.
(18) Kelleher, N. L.; Nicewonger, R. B.; Begley, T. P.; McLafferty, F. W. *J. Biol. Chem.* **1997**, *272*, 32215−32220.
(19) Kelleher, N. L.; Taylor, S. V.; Grannis, D.; Kinsland, C.; Chiu, H. J.; Begley, T. P.; McLafferty, F. W. *Protein Sci.* **1998**, *7*, 1796−1801.
(20) Lavanant, H.; Derrick, P. J.; Heck, A. J.; Mellon, F. A. *Anal. Biochem.* **1998**, *255*, 74−89.
(21) Kelleher, N. L.; Lin, H. Y.; Valaskovic, G. A.; Aaserud, D. J.; Fridriksson, E. K.; McLafferty, F. W. *J. Am. Chem. Soc.* **1999**, *121*, 806−812.
(22) Maier, C. S.; Yan, X.; Harder, M. E.; Schimerlik, M. I.; Deinzer, M. L.; Pasa-Tolic, L.; Smith, R. D. *J. Am. Soc. Mass Spectrom.* **2000**, *11*, 237−243.
(23) Cancilla, M. T.; Penn, S. G.; Lebrilla, C. B. *Anal. Chem.* **1998**, *70*, 0, 663−672.
(24) Solouki, T.; Reinhold: B. B.; Costello, C. E.; O'Malley, M.; Guan, S.; Marshall, A. G. *Anal. Chem.* **1998**, *70*, 857−864.
(25) Cancilla, M. T.; Wong, A. W.; Voss, L. R.; Lebrilla, C. B. *Anal. Chem.* **1999**, *71*, 3206−3218.

10.1021/ac0489824 CCC: $30.25
Published on Web 12/03/2004

However, a disadvantage of CID is the decrease in both the degree and efficiency of dissociation with increasing mass for the same charge-state ions.[31,32] In addition, FTICR-MS has fixed magnetic fields and effective maximum cyclotron radii, which limit the ion's kinetic energy.[33] In general, multiple stages of CID (MS^n, $n > 2$) are often required for detailed structural analysis of large oligosaccharides. Because the mass-to-charge (m/z) values of the precursor ions vary widely through the sequential MS/MS stages, optimization of the CID parameters for each m/z becomes a time-consuming process. With each tandem MS event, the fragment ion intensities and signal-to-noise ratios are decreased due to ion loss.[33]

Infrared multiphoton dissociation (IRMPD) has shown great promise as an alternative to CID in ion trapping mass spectrometers. IRMPD is a general dissociation technique because all organic molecules tend to readily absorb IR photons. One advantage of IRMPD compared to CID is that no collision gas is needed thereby shortening the analysis time in FTICR MS. Moreover, photon absorption does not cause translational excitation of ions as does CID, thus minimizing losses of ions due to ejection or ion scattering. Since both precursor and fragment ions can absorb IR photons, more extensive fragmentation pathways can be observed. IRMPD also provides for on-axis fragmentation (for more efficient observation of product ions), good control over ion excitation energy, and minimal mass discrimination. IRMPD has been extensively utilized with FTICR-MS for the structural characterization of intact proteins,[34−37] peptides,[38−42] DNA, and nucleotides. [43−45] Recently, this laboratory performed IRMPD on the a small group of oligosaccharides with different alkali metal coordinators.[46]

In the present study, we performed IRMPD experiments on a large number of mucin-type oligosaccharides including neutral, sialylated, and sulfated oligosaccharides. They are released in the alditol form from the outer jelly layer of amphibian eggs and are known to play essential roles in fertilization such as recognition, sperm capacitation, protection of eggs against pathogens, and prevention of polyspermy.[47] Thus far, anionic oligosaccharides have not been studied by IRMPD. It is also shown that the fragmentation efficiency of IRMPD is increased with the sizes of oligosaccharides. IRMPD provides not only a faster and simpler tandem mass spectrometry technique but also a more efficient dissociation method than CID for the structural elucidation of oligosaccharides.

EXPERIMENTAL SECTION

Materials. O-Linked oligosaccharide alditols were isolated from egg jelly glycoproteins of three different South African toad, *Xenopus laevis*, *Xenopus tropicalis,* and *Xenopus borealis*. The procedure is described in previous publications.[4,8,48] The matrix, 2,5-dihydroxybenzoic acid (DHB), was obtained from Aldrich Chemical Co. (Milwaukee, WI). All reagents were purchased in the highest purity and used without further purification.

Mass Spectrometry. All experiments were performed on a commercial matrix-assisted laser desorption/ionization Fourier transform ion cyclotron resonance mass spectrometry (MALDI-FTICR MS) instrument (Ion Spec, Irvine, CA). This instrument is equipped with a 7.0-T shielded, superconducting magnet and a Nd:YAG laser operating at 355 nm. The MALDI sample was prepared by concentrating 1−20 μL of an HPLC fraction directly on the probe. One microliter of 0.4 M DHB in acetonitrile/water (50:50) was added as the matrix. For the positive mode, 1 μL of 0.1 M NaCl in acetonitrile/water solution (50:50) was added to the probe tip to enrich the Na^+ concentration and produce primarily sodiated species.

Sustained Off-Resonance Irradiation Collision-Induced Dissociation (SORI-CID). All CID experiments were performed in the off-resonance mode. The desired ion was isolated in the ion cyclotron resonance (ICR) cell by the use of an arbitrary waveform generator. The ions were excited +1000 Hz of their cyclotron frequency for 1000 ms at 2−8 V (base to peak) depending on the desired level of fragmentation and the size of oligosaccharides. Two argon pulses were used during the CID event to maintain a pressure of 10^{-5} Torr.

Infrared Multiphoton Dissociation. A continuous-wave Parallax CO_2 laser (Waltham, MA) with 20-W maximum power and 10.6-μm wavelength was installed at the rear of the magnet and is used to provide the photons for IRMPD. The laser beam diameter is 6 mm as specified by the manufacturer. To ensure complete irradiation of the ion cloud, the laser beam was expanded to ~12 mm by means of a 2× beam expander (Synrad, Mukilteo, WA). To perform IRMPD experiments, modifications were carried

(26) Gaucher, S. P.; Cancilla, M. T.; Phillips, N. J.; Gibson, B. W.; Leary, J. A. *Biochemistry* **2000**, *39*, 12406−12414.
(27) Penn, S. G.; Cancilla, M. T.; Lebrilla, C. B. *Int. J. Mass Spectrom.* **2000**, *196*, 259−269.
(28) Hettich, R. L.; Stemmler, E. A. *Rapid Commun. Mass Spectrom.* **1996**, *10*, 321−327.
(29) Flora, J. W.; Hannis, J. C.; Muddiman, D. C. *Anal. Chem.* **2001**, *73*, 1247−1251.
(30) Pastor, S. J.; Wilkins, C. L. *Int. J. Mass Spectrom. Ion Processes* **1998**, *175*, 81−92.
(31) Biemann, K.; Martin, S. A. *Mass Spectrom. Rev.* **1987**, *6* (1), 1−76.
(32) Hunt, D. F.; Shabanowitz, J.; Yates, J. R., III; Griffin, P. R.; Zhu, N. Z. In *Methods in Protein Sequence Analysis*; Wittmann-Liebold, B., Ed.; Spring Verlag: New York, 1989; pp 183−190.
(33) Williams, E. R.; Furlong, J. P.; McLafferty, F. W. *J. Am. Soc. Mass Spectrom.*, **1990**, *1*, 288−294.
(34) Little, D. P.; Speir, J. P.; Senko, M. W.; O'Connor, P. B.; McLafferty, F. W. *Anal. Chem.* **1994**, *66*, 2809−2815.
(35) Mortz, E.; O'Connor, P. B.; Roepstorff, P.; Kelleher, N. L.; Wood, T. D.; McLafferty, F. W.; Mann, M. *Proc. Natl. Acad. Sci. U.S.A.* **1996**, *93*, 8264−8267.
(36) Li, W.; Hendrickson, C. L.; Emmett, M. R.; Marshall, A. G. *Anal. Chem.* **1999**, *71*, 4397−4402.
(37) Meng, F.; Cargile, B. J.; Patrie, S. M.; Johnson, J. R.; McLoughlin, S. M.; Kelleher, N. L. *Anal. Chem.* **2002**, *74*, 2923−2929.
(38) Jockusch, R. A.; Paech, K.; Williams, E. R. *J. Phys. Chem. A* **2000**, *104*, 3188−3196.
(39) Masselon, C.; Anderson, G. A.; Harkewicz, R.; Bruce, J. E.; Pasa-Tolic, L.; Smith, R. D. *Anal. Chem.* **2000**, *72*, 1918−1924.
(40) Flora, J. W.; Muddiman, D. C.; *Anal. Chem.* **2001**, *73*, 3305−3311.
(41) Hakansson, K.; Cooper, H. J.; Emmett, M. R.; Costello, C. E.; Marshall, A. G.; Nilsson, C. L. *Anal. Chem.* **2001**, *73*, 4530−4536.
(42) Li, L.; Masselon, C. D.; Anderson, G. A.; Pasa-Tolic, L.; Lee, S. W.; Shen, Y.; Zhao, R.; Lipton, M. S.; Conrads, T. P.; Tolic, N.; Smith, R. D. *Anal. Chem.* **2001**, *73*, 3312−3322.
(43) Little, D. P.; McLafferty, F. W. *J. Am. Chem. Soc.* **1995**, *117*, 6783−6784.
(44) Little, D. P.; Aaserud, D. J.; Valaskovic, G. A.; McLafferty, F. W. *J. Am. Chem. Soc.* **1996**, *118*, 9352−9359.
(45) Little, D. P.; McLafferty, F. W. *J. Am. Soc. Mass Spectrom.* **1996**, *7*, 209−210.
(46) Xie, Y.; Lebrilla, C. B. *Anal. Chem.* **2003**, *75*, 1590−1598.
(47) Wyrick, R. E.; Nishihara, T.; Hedrick, J. L. *Proc. Natl. Acad. Sci. U.S.A.* **1974**, *71*, 2067−2071.
(48) Tseng, K.; Xie, Y.; Seely, J.; Hedrick, J. L.; Lebrilla, C. B. *Glycoconjugate J.* **2001**, *18*, 309−320.

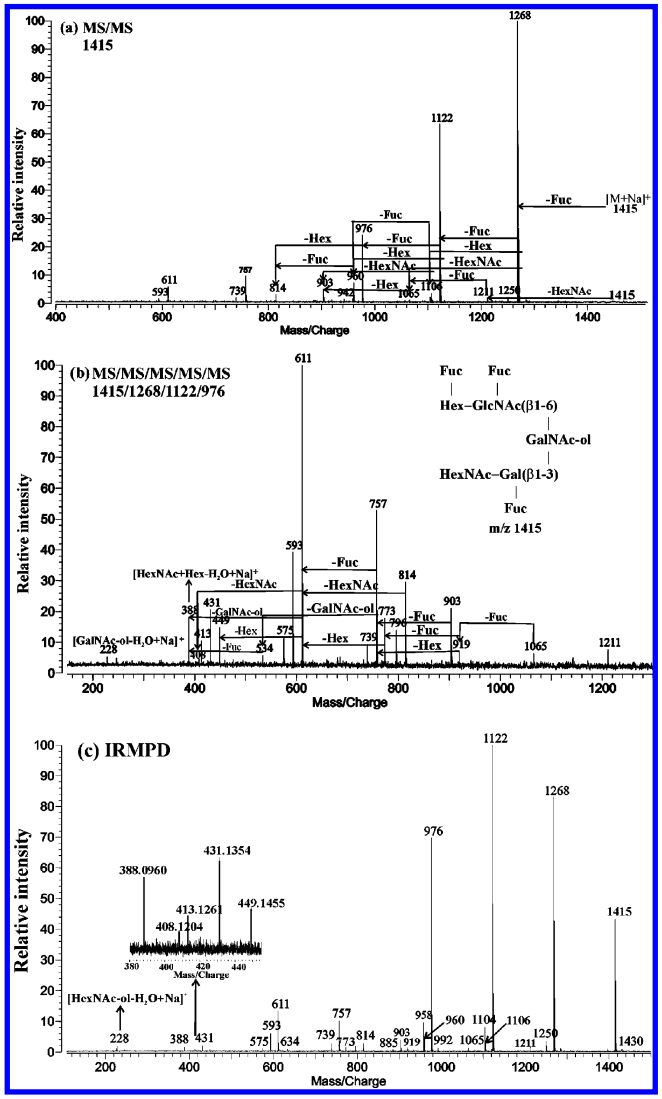

Figure 1. CID and IRMPD mass spectra of neutral oligosaccharide alditol XT-1415. (a) MS^2 CID spectrum. (b) MS^5 CID spectrum (m/z 1415 → 1268 → 1122 → 976). (c) IRMPD mass spectrum of the quasi-molecular ion. All representative fragment ions present in the multistage CID spectra are observed in the IRMPD experiment.

out on the ICR cell as described in detail previously.[46,49] The laser was aligned and directed to the center of the ICR cell through a BaF_2 window (Bicron Corp., Newbury, OH). The laser was operated at an output of ~12 W. Photon irradiation time was optimized to produce the greatest number and abundance of fragment ions (typically 400−800 ms). For comparison, CID and IRMPD were achieved under similar experimental conditions with the precursor ion isolated before activation using an arbitrary waveform generator.

RESULTS

Comparison of CID and IRMPD of Mucin-Type Oligosaccharides. In this study, we examined the CID and IRMPD mass spectra of a variety of oligosaccharide alditols in order to compare the structural information obtained from both. Figure 1a and 1b show multi-stage CID spectra of a neutral oligosaccharide alditol XT-1415 from *X. tropicalis*. The composition of the oligosaccharide was predicted from the exact mass at m/z 1414.521 (theoretical m/z 1414.533) to be 2 Hex, 3 Fuc, and 3 HexNAc. The dominant fragmentation pathways in the CID spectra correspond to glycosidic bond cleavage (mainly y and b ions[50]) from the nonreducing end to the reducing end. The MS^2 of the parent ion provided high ion abundances of high-mass ions as shown in Figure 1a. More energetic CID conditions, such as higher rf amplitude or longer excitation time, could be used to produce the low-mass fragment peaks at the expense of the high-mass fragments and the overall signal intensity. Multiple stages of tandem mass spectrometry experiments are generally necessary to yield the last residue. For example, MS^5 was employed to compound XT-1415 in order to obtain monosaccharide residue corresponding to m/z 228.084 ($[HexNAC\text{-}ol - H_2O + Na]^+$). Loss of Fuc ($m/z$ 1268) and HexNAc (m/z 1211) from the quasi-molecular ion, followed by loss of two and three consecutive fucoses (m/z 1268 → 1122 → 976 and m/z 1211 → 1065 → 919 → 773, respectively) were observed, indicating that three Fuc and one HexNAc were nonreducing termini. The fragment ions on the MS^5 spectra corresponding to m/z 611, 449, 431, 413, and 408 identify the presence of the known trisaccharide core, Gal(β1−3)[GlcNAc-(β1−6)]GalNAc-ol,[8,48] which is also the most common core structure for mucin-type oligosaccharides from the jelly coat of amphibians.[51] Based on the CID data, the connectivity of XT-1415 was deduced and inset in Figure 1b. Note the decrease in S/N between Figure 1a and b as a consequence of ion loss due to ion scattering during multiple stages of MS.

Figure 1c shows the IRMPD spectrum of XT-1415. In Figure 1c, the ions ranging from the precursor ion to the terminal monosaccharide residue (m/z 228) corresponding to $[HexNAc\text{-}ol - H_2O + Na]^+$ were readily observed. It was noted that all informative peaks appearing in CID spectra were clearly shown in the IRMPD spectrum. The group of fragment ions representing the trisaccharide core (inset in Figure 1c) was also similar to those produced by CID. IRMPD yielded nearly identical fragment ions as CID for this oligosaccharide and corresponded primarily to glycosidic bond cleavage (y and b ions). A single MS/MS event in CID gives a higher abundance of high-mass ions because CID selectively energizes primarily the parent ion, whereas IRMPD deposits energy into all ions, including precursor and fragment ions. The advantages of IRMPD over CID are readily illustrated in this example—IRMPD is faster, requiring only a single MS/MS experiment resulting in greater sensitivity as evidenced by the signal-to-noise ratio.

In the present study, all IRMPD experiments were performed at constant laser power with the irradiation time varied to affect the degree of fragmentation. In a previous study by Shi et al. on the IRMPD of the glycoconjugate saccharmonicins,[52] the degree of fragmentation was varied by varying the laser power. IRMPD mass spectra obtained at varying laser powers were combined to yield the complementary structural information. Varying the irradiation time provided a relatively more precise control of energy. At short irradiation times, the product ions were mostly limited to larger fragment ions. As the irradiation times were

(49) Xie, Y.; Schubothe, K. M.; Lebrilla, C. B. *Anal. Chem.* **2003**, *75*, 160−164.
(50) Domon, B.; Costello, C. E. *Glycoconjugate J.* **1988**, *5*, 397−409.
(51) Guerardel, Y.; Kol, O.; Maes, E.; Lefebvru, T.; Boilly, B.; Davril, M.; Strecker, G. *Biochem. J.* **2001**, *352*, 449−463.
(52) Shi, D.-H.; Hendrickson, C. L.; Marshall, A. G.; Siegel, M. M.; Kong, F.; Carter, G. T *J. Am. Soc. Mass Spectrom.* **1999**, *10* (12), 1285−1290.

increased, these ions were further dissociated, shifting the intensities to smaller product ions. Laser times were optimized using experiments at varying irradiation length in order to obtain the most informative fragments. The IRMPD conditions are similar for all oligosaccharides with some minor variation in irradiation times. For CID, each mass had to be optimized individually in terms of the isolation, the excitation, and the collision gas pressure.

Tandem MS data based on CID were previously used to determine linkage and anomeric character by developing a catalog of fragmentation patterns distinct for specific structural motifs.[8,48] The catalog was used to determine unknown structures in an oligosaccharide library. The catalog library approach has been extensively employed to elucidate the complete structures of oligosaccharides found in *X. laevis*.[8,48] A catalog consisting of 5 structural motifs was constructed from tandem MS studies of 12 oligosaccharides whose structures were initially determined by NMR.[53] Each motif yielded a distinct fragmentation pattern, which can be identified solely from the CID spectra. The presence of the motifs were confirmed by exoglycosidase digestions.[54]

Examples of the motifs and their fragmentation patterns are illustrated in Figure 2 and Figure 3. Motif ii and motif iii in structure XL-1065-1 and XL-1065-2 are shown in Figure 2a and Figure 3a, respectively. The two structures have same composition and connectivity (the nonspecific connection of the residues). The only difference is found in one linkage, Gal(α1−4)[Fuc(α1−2)]-Gal(β1−3) for XL-1065-1 and Gal(β1−3)[Fuc(α1−2)]Gal(β1−3) for XL-1065-2. Each structural motif, ii and iii, has a unique CID fragmentation pattern. Motif ii has characteristic signals corresponding to significant losses of both Hex (162amu) and Fuc (146amu) from $[M + Na]^+$. Motif iii is characterized by the presence of the m/z 347 observed in Figure 3b, which is characteristic of the Gal(β1−3)Gal(β1−3) fragment coordinated to Na^+. It is also characterized by the loss of fucose and the weak loss of Hex from the quasi-molecular ion $[M + Na]^+$ in Figure 3a. Both structures contain motif i, a trisaccharide core, which is characterized by peaks of m/z 611, 449, 431, 413, 408, and 390 in CID spectra. Complete structures can be deduced by piecing the two motifs together (insets in Figure 2b and Figure 3b, respectively). However, to obtain the complete structures, MS^4 was necessary for both compounds.

In the corresponding IRMPD spectra (Figure 2c and Figure 3c), the fragments to the final residue (m/z 228) were obtained from a MS^2 experiment. As stated previously, IRMPD followed essentially the same dissociation pathways as CID yielding the same fragment ions. Motifs i, ii, and iii were readily identified in the IRMPD spectrum using the same characteristic fragment ions. The structures of the two compounds were therefore readily elucidated with an MS^2 experiment. With minimal tuning, IRMPD can be used to replace multiple stages of MS to yield characteristic fragment ions that can identify specific structural motifs. We find that similar irradiation conditions can be used for nearly all the oligosaccharides in both the positive and the negative modes.

IRMPD of Sialylated and Sulfated Oligosaccahrides. Sialylated oligosaccharides are important components of amphibian egg jelly and play key roles in cell−cell interactions. The sialic acid (Neu5Ac) is generally labile in MALDI-MS and is readily cleaved during ionization and tandem MS experiments. In the negative mode, IRMPD yields only a single product (m/z 290) corresponding to the deprotonated sialic acid residue (data not shown). To stabilize the sialic acid, methyl esterification was employed and the compound analyzed in the positive mode. The IRMPD of a methyl-esterified sialylated oligosaccharide revealed the complete connectivity information of XT-1024 (Figure 4, m/z 1024.386, 1 Hex, 1 Fuc, 2 HexNAc, and 1 Neu5Ac). The peak at m/z 1062.397 corresponded to the methyl-derivatized quasi-molecular ion with sodium doping in the positive mode. The losses of Fuc (m/z 916) and esterified sialic acid (m/z 757) from quasi-molecular ion indicated that Fuc and Neu5Ac were present at the nonreducing ends. The peak at m/z 246.095 was the reducing terminus in its sodiated alditol form. The presence of m/z 449.174 and 388.122 yielded the [HexNAc − HexNAc-ol] and [Hex − HexNAc], respectively. Based on these fragment ions, the sequence was obtained (inset in Figure 4).

An example of structural analysis of a sulfated oligosaccharide XT-1852 with IRMPD is illustrated (Figure 5) in negative mode. This singly sulfated oligosaccharide (m/z 1851.621) is composed of 3 Hex, 2 Fuc, and 4 HexNAc units. There were some initial

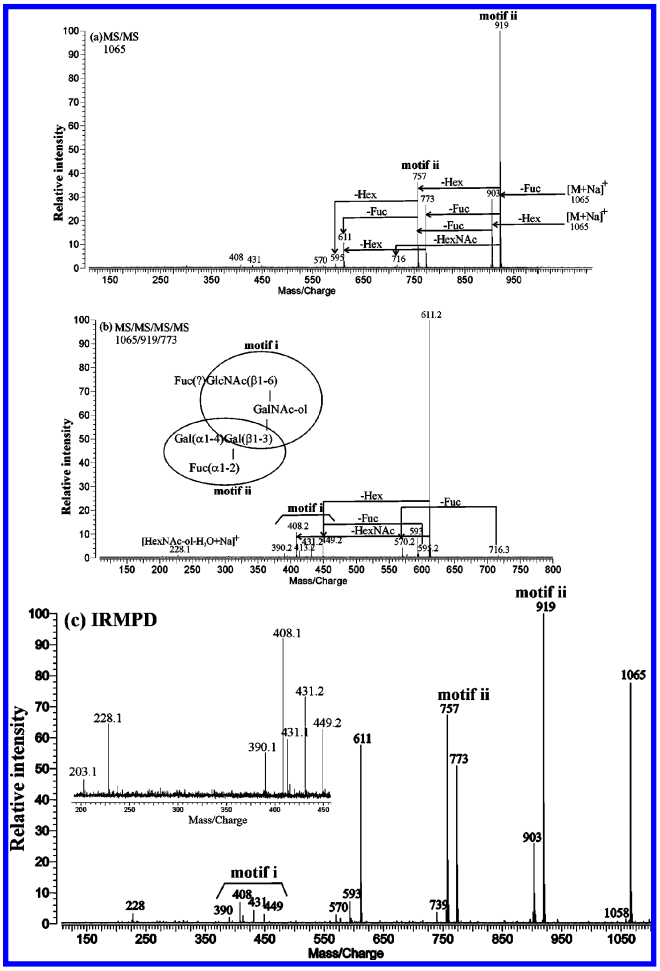

Figure 2. CID and IRMPD mass spectra of neutral oligosaccharide XL-1065−1. (a) MS^2 CID spectrum. (b) MS^4 CID spectrum (m/z 1065 → 919 → 773). (c) IRMPD spectrum of the quasi-molecular ion. All representative fragment ions present in the multistage CID spectra are observed in the IRMPD experiment.

(53) Strecker, G.; Wieruszeski, J.-M.; Plancke, Y.; Boilly, B. *Glycobiology* **1995**, *5*, 137−46.
(54) Xie, Y.; Tseng, K.; Hedrick, J. L.; Lebrilla, C. B. *J. Am. Soc. Mass Spectrom.* **2002**, *12*, 877−884.

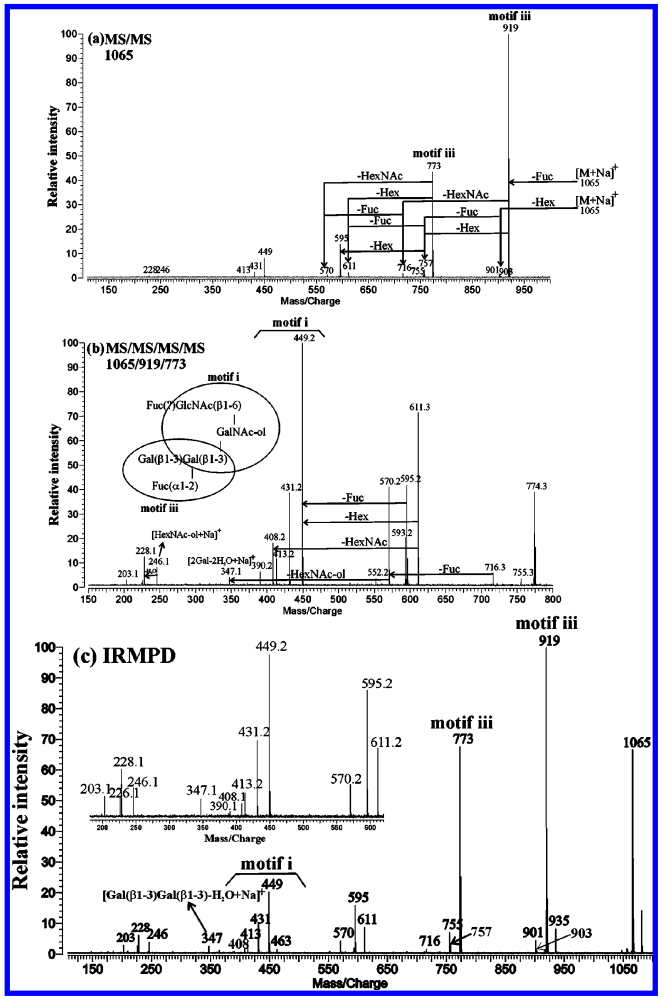

Figure 3. CID and IRMPD mass spectra of neutral oligosaccharide XL-1065−2.(a) MS^2 CID spectrum. (b) MS^4 CID spectrum (m/z 1065 → 919 → 773). (c) IRMPD spectrum of the quasi-molecular ion. All representative fragment ions present in the multistage CID spectra are observed in the IRMPD experiment.

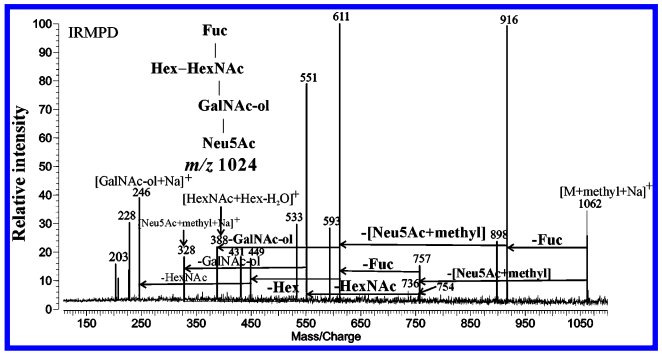

Figure 4. IRMPD spectrum of sialylated oligosaccharide XT-1024 after methyl esterification. The spectrum is obtained in the positive mode with $[M + Na]^+$.

concerns that IRMPD of the sulfated oligosaccharides would simply yield the single sulfated residue. However, the tandem MS of sulfated oligosaccharides produced fragments with representative cleavage from every glycosidic bond, unlike the underivatized sialylated oligosaccharides. All fragment ions contained the sulfate group, providing the connectivity of carbohydrate chain. As shown in Figure 5, IRMPD yielded extensive fragments ranging from the loss of one residue to the last charge-carrying residue

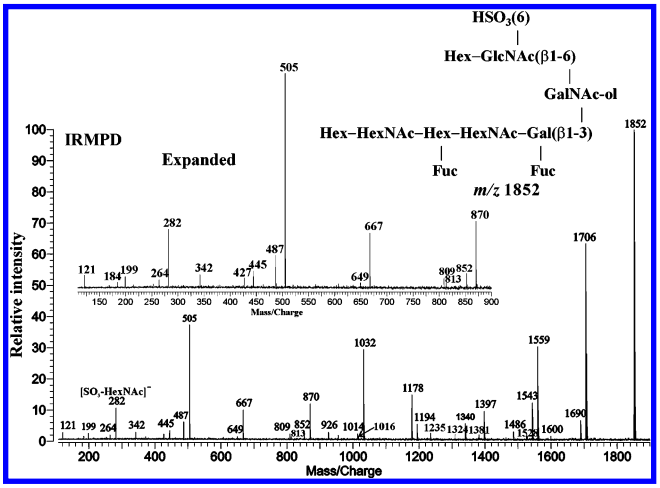

Figure 5. IRMPD spectrum of sulfated oligosaccharide XT-1852 in the negative mode. The quasi-molecular ion corresponds to $(M - H)^-$. Representative fragments are found for every linkage.

corresponding to m/z 282.036 ($[HexNAc - SO_3]^-$). The fragment ions with m/z 1706 and 1690 corresponded to the loss of Fuc and Hex from the quasi-molecular ions, respectively, and indicated that both Fuc and Hex were at the nonreducing termini. The absence of the loss of a HexNAc-ol group from the quasi-molecular ion suggested the oligosaccharide was branched at the alditol end. The ions with m/z 505.135 and 282.036 corresponded to $[SO_3 - HexNAc - HexNAc\text{-}ol]^-$ and $[HexNAc - SO_3]^-$, respectively. The fragment ion with m/z 667.187 suggested one additional Hex attached to HexNAc-ol. The above three peaks identified the presence of a trisaccharide core, Gal(β1−3)[SO_3-GlcNAc(β1−6)]-GalNAc-ol, with the sulfate group located on the GlcNAc of the core. This core structure is common among the sulfated oligosaccharides found in the jelly coat of amphibian eggs.[51] The fragment ion with m/z 198.998 corresponded to the $^{0,2}A_1$ cross-ring cleavage of terminal, sulfated GlcNAc group. The ion is diagnostic for locating the sulfate group and indicates it to be linked to the C-4 or C-6 of the GlcNAc.[55] NMR studies have shown that the sulfate group in similar compounds was exclusively located on the C-6 of GlcNAc of the core for amphibian eggs.[51] The group of ions at m/z 667, 505, 282, and 199 can be considered as characteristic peaks of the motif Gal(β1−3)[SO_3(6) − GlcNAc(β1−6)]GalNAc-ol. This motif and the corresponding fragmentation pattern are found in most *X. tropicalis* sulfated oligosaccharides including XT-813−1, XT-1016−1, XT-1121−1, XT-1178−1, XT-1219−1, XT-1324−1, XT-1528−1, XT-1690−1, and XT-1731−1.

The O-linked oligosaccharides examined by IRMPD in this study are listed in Chart 1 and Chart 2. A total of 39 structures were elucidated and include neutral (Chart 1) and anionic composed of sialylated and sulfated oligosaccharides (Chart 2). Some are known oligosaccharides, while others are unknown with the connectivity determined by IRMPD. The wide breadth of compounds indicates that IRMPD is a general dissociation method for many types of oligosaccharides.

Dependence of IRMPD on Increasing Size of Oligosaccharides. High-mass ions are not efficiently dissociated by CID. The fragmentation efficiencies of large molecules are limited by

(55) Thomsson, K. A.; Karlsson, H.; Hansson, G. C. *Anal. Chem.* **2000**, *72*, 4543−4549.

Chart 1. Neutral Oligosaccharides Elucidated by IRMPD

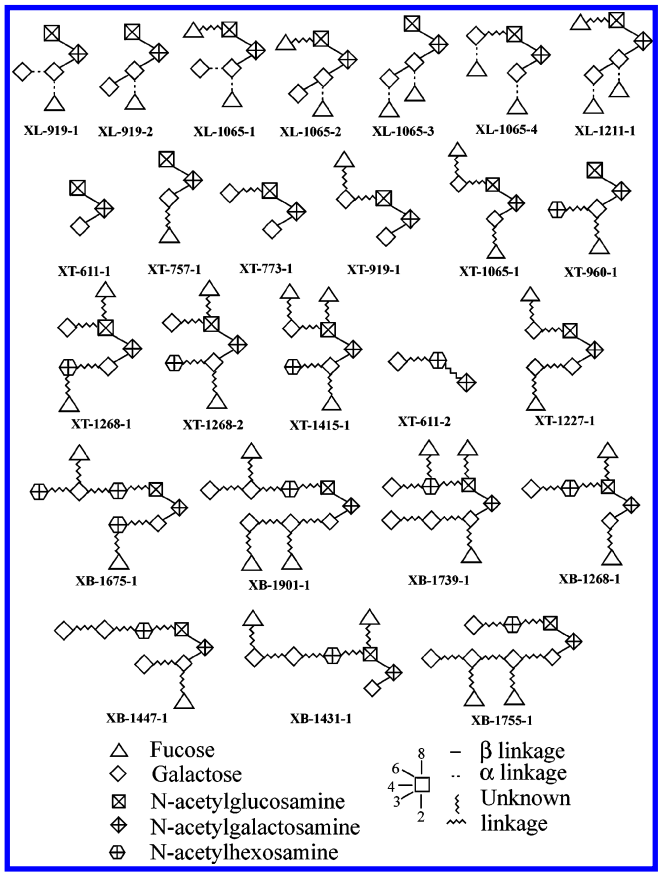

Chart 2. Anionic Oligosaccharides Elucidated by IRMPD

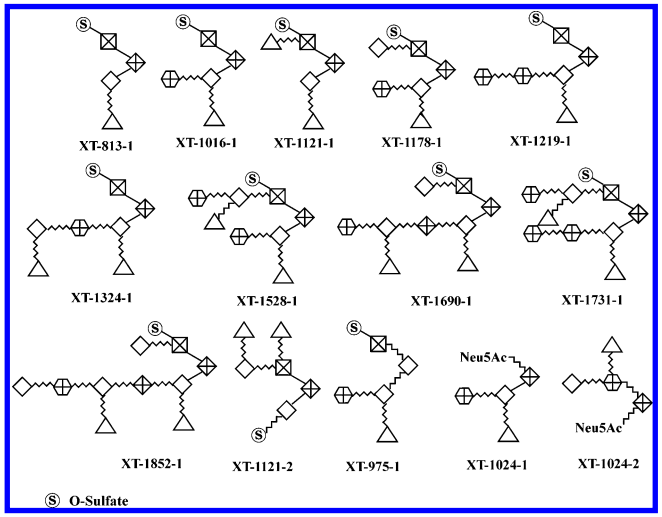

both the decrease in the center-of-mass collision energy, associated with the increasing precursor ion mass, and the dimension of the ICR cell.[33] Furthermore, when the parent ions are translationally excited, the product ions may diffuse radially due to magnetron orbit expansion.[56] This results in the loss of lower mass ions with each subsequent tandem MS event. IRMPD can access these smaller ions through secondary dissociation processes as

(56) Francl, T. J.; Fukuda, E. K.; McIver, R. T., Jr. *Int. J. Mass Spectrom. Ion Processes* **1983**, *50* (1−2), 151−67.

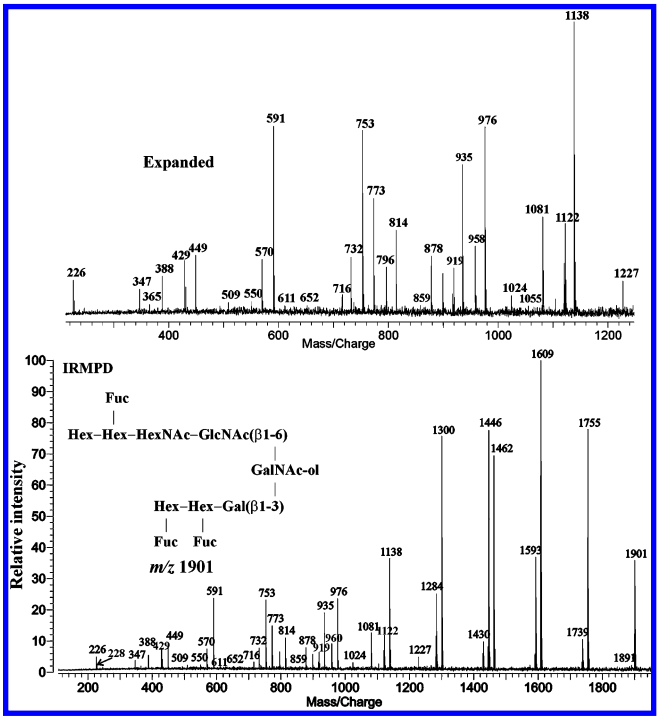

Figure 6. IRMPD mass spectrum of neutral oligosaccharide XB-1901. Fragment ions corresponding to every glycosidic bond cleavage are observed in the MS^2 experiment.

the fragments are produced in the center of cell within the degradative volume of the radiation beam.[42,43,57] For example, a neutral oligosaccharide alditol XB-1901 (m/z 1900.692) from *X. borealis* composed of 5 Hex, 3 Fuc, and 3 HexNAc units could not be fully sequenced by CID as the ion required over five stages of tandem MS to obtain the final residues. At that point, signal was lost and no further sequence fragments were observed. However, as shown by the IRMPD spectra in Figure 6, the ions ranging from the parent ion to final monosaccharide residue (m/z 228.084) corresponding to $[GalNAc\text{-}ol - H_2O + Na]^+$ were readily observed. The loss of Fuc (m/z 1755) and Hex (m/z 1739) from the quasi-molecular ion indicated that both Fuc and Hex were at the nonreducing end terminus. The ultrahigh-mass resolution and high-mass accuracy of FTMS helped minimize the complexity, allowing complete sequencing of the oligosaccharide. The complete connectivity (inset) of this compound was deduced based solely on the IRMPD spectra.

A systematic study was performed to determine whether the IRMPD efficiency correlated with the sizes of oligosaccharides. Five neutral oligosaccharides ranging from a trisaccharide to an octasaccharide were chosen. All have the same core structure corresponding to Gal(β1−3)[GlcNAc(β1−6)]GalNAc-ol. The IRMPD of the five compounds were achieved under similar experimental condition including laser irradiation period and laser power. The bar graph in Figure 7 shows the ratios of the sum of all fragments to the total ion intensity in the IRMPD mass spectra of the five oligosaccharides after 800 ms of irradiation time. The fragmentation increases dramatically with increasing size. The quasi-molecular ion of the octasaccharide (m/z 1415) was depleted completely under the irradiation conditions, while ~90% of the trisaccharide (m/z 611) did not decompose. It was also found that

(57) Shen, J.; Brodbelt, J. S. *Analyst* **2000**, *125* (4), 641−650.

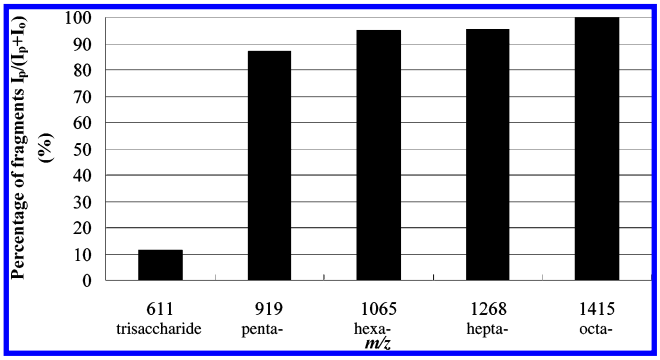

Figure 7. Percentages of fragments as a function of the oligosaccharides sizes under identical IRMPD experimental conditions. Irradiation period is 800 ms with 12 W of laser power.

no fragments were observed with an irradiation period of less than 300 ms for any of the oligosaccharide, indicating an induction period prior to the onset of decomposition. The high fragmentation efficiency of high-mass ions may attribute to the rapid increase of the density of vibrational states with increasing molecular sizes.

CONCLUSION

IRMPD offers a general method for performing tandem MS and obtaining structurally important fragment ions of oligosaccharides. They yield abundant ions for neutral, sialylated, and sulfated O-linked oligosaccharides. The ions produced are nearly identical to CID with a few minor exceptions. For example, a cross-ring cleavage product was observed with sulfated oligosaccharides that was absent in the CID spectra. IRMPD has several advantages over CID. There is very little ion loss during tandem MS events as collision gas is not introduced into the analyzer cell. The absence of collision gas also significantly increases the repetition rate as the chamber is no longer pumped down. IRMPD is well suited for high-mass ions that are not fully elucidated by CID. In our experience, CID works well for ions below m/z 1400 but becomes impractical for oligosaccharide ions above 1400. IRMPD, on the other hand, works well for ions with m/z above 500 and increases in fragmentation efficiency as the ions increase beyond m/z 2000. IRMPD will therefore find wide application particularly with oligosaccharides and is even preferable to CID.

ACKNOWLEDGMENT

Funding provided by the National Science Foundation and the National Institute of Health is gratefully acknowledged. The authors thank Crystal Kirmiz for her help with sample preparation.

Received for review July 12, 2004. Accepted October 22, 2004.

AC0489824